International Journal of Pharmaceutics 363 (2008) 170–176

Contents lists available at ScienceDirect

International Journal of Pharmaceutics

journal homepage: www.elsevier.com/locate/ijpharm

Pharmaceutical Nanotechnology

Novel method of doxorubicin–SPION reversible association for magnetic drug targeting

E. Munnier[a,b], S. Cohen-Jonathan[a,b], C. Linassier[a,b,c], L. Douziech-Eyrolles[a,b], H. Marchais[a,b], M. Soucé[a,b], K. Hervé[a,b], P. Dubois[a,b], I. Chourpa[a,b,*]

[a] Université François-Rabelais, Faculté de Pharmacie, "Focalisation magnétique d'agents anticancéreux", Tours F-37200, France
[b] Institut Fédératif de Recherche 135 "Imagerie Fonctionnelle", Tours F-37000, France
[c] CHRU Bretonneau, Service d'Oncologie Médicale, Tours F-37000, France

ARTICLE INFO

Article history:
Received 4 March 2008
Received in revised form 7 July 2008
Accepted 8 July 2008
Available online 16 July 2008

Keywords:
Doxorubicin
Nanoparticles
Controlled release/delivery
Magnetic drug targeting
Cancer cell

ABSTRACT

A new method of reversible association of doxorubicin (DOX) to superparamagnetic iron oxide nanoparticles (SPION) is developed for magnetically targeted chemotherapy. The efficacy of this approach is evaluated in terms of drug loading, delivery kinetics and cytotoxicity *in vitro*. Aqueous suspensions of SPION (ferrofluids) were prepared by coprecipitation of ferric and ferrous chlorides in alkaline medium followed by surface oxidation by ferric nitrate and surface treatment with citrate ions. The ferrofluids were loaded with DOX using a pre-formed DOX–Fe^{2+} complex. The resulting drug loading was as high as 14% (w/w). This value exceeds the maximal loading known from literature up today. The release of DOX from the nanoparticles is strongly pH-dependent: at pH 7.4 the amount of drug released attains a plateau of ~85% after 1 h, whereas at pH 4.0 the release is almost immediate. At both pH, the released drug is iron-free. The *in vitro* cytotoxicity of the DOX-loaded SPION on the MCF-7 breast cancer cell line is similar to that of DOX in solution or even higher, at low-drug concentrations. The present study demonstrates the potential of the novel method of pH-sensitive DOX–SPION association to design novel magnetic nanovectors for chemotherapy.

1. Introduction

The anthracycline antibiotic adriamycin or doxorubicin (DOX, Fig. 1) is a highly efficient antineoplastic agent commonly used in the treatment of a variety of cancers like leukaemia, ovarian cancer and especially late stage breast cancer (Hoke et al., 2005). The clinical use of DOX is limited by the resistance developed by cancer cells and by strong side effects, namely a dose-dependent cardiotoxicity (Bast et al., 2007; Petit, 2004).

Drug targeting, that is drug delivery to the tumor site, helps prevent side effects and increase cytotoxicity of doxorubicin. Several principles of drug targeting are being investigated, for instance molecular coupling of the anticancer agent to specific molecules like low-density lipoproteins (Lo et al., 2002) or monoclonal antibodies (Inoh et al., 2006) which interact with specific receptor(s) in the tumor.

Another possible approach for drug targeting is the delivery using an aqueous suspension of magnetic nanoparticles retained in a tumor by application of an external magnetic field (magnetic drug targeting) (Lübbe et al., 2001; Torchilin, 2006). The superparamagnetic iron oxide nanoparticles (SPION, Neuberger et al., 2005) are particularly interesting, since they are devoid of magnetic remanence due to their very small size (often below 10 nm). In the last years, SPION-based ferrofluids have been developed as contrast agents for magnetic resonance imaging (MRI) and as heating intermediates for magnetic hyperthermia (Alexiou et al., 2006; Corot et al., 2006; Duguet et al., 2006; Moghimi and Kissel, 2006; Neuberger et al., 2005). The enhanced interest of the SPION–drug associates is related to the potentially combined functions of targeted therapy and diagnosis (Duguet et al., 2006; Neuberger et al., 2005). The association drug–SPION for magnetic drug targeting can be realized either by direct binding to the iron oxide surface or by encapsulating both drug and SPION within a biodegradable polymeric matrix (Berry and Curtis, 2003; Duguet et al., 2006; Jain et al., 2005; Neuberger et al., 2005; Ngaboni Okassa et al., 2007).

The drug loading values obtained with direct drug–SPION binding are generally comprised between 0.5 and 12% (w/w) (Alexiou et al., 2000; Jain et al., 2005; Lübbe et al., 1996a,b; Mykhaylyk et al., 2005; Rudge et al., 2000; Zhang and Misra, 2007). Direct drug binding to magnetic nanoparticles can be achieved by either covalent bonds or ionic interactions (Alexiou et al., 2000; Duguet et al.,

* Corresponding author at: Laboratoire de Chimie Analytique, UFR de Pharmacie, 31 avenue Monge, Tours F-37200, France. Tel.: +33 247 367162; fax: +33 247 367270.
E-mail address: chourpa@univ-tours.fr (I. Chourpa).

0378-5173/$ – see front matter © 2008 Elsevier B.V. All rights reserved.
doi:10.1016/j.ijpharm.2008.07.006

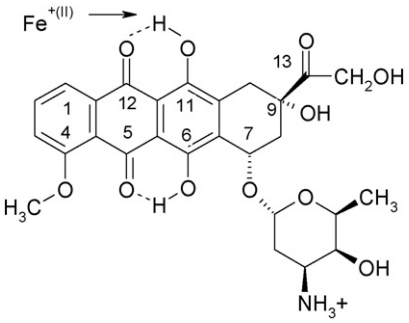

Fig. 1. Structural formula of doxorubicin (DOX) with the site of preferential Fe^{2+} ion binding in an aqueous buffer pH 7.6: iron replaces one phenolic hydrogen at position 11.

2006; Lübbe et al., 1996a,b). In contrast to covalent binding, ionic adsorption is easily reversible since it depends on ionic strength and pH. As a result, the kinetics of drug release from ionic systems are expected to be faster than in the case of covalent binding. Nanoparticular magnetic fluids with ionically adsorbed epirubicin have been reported to increase the drug content in tumor tissue (Lübbe et al., 1996a,b), thus demonstrating magnetic drug targeting feasibility. In that work, epirubicin was adsorbed due to the interaction between the positively charged amino sugar of the drug and the particle surface previously functionalized with anionic phosphate groups.

In the present article, we propose and evaluate a new approach of binding DOX to the SPION surface using a pre-formed complex of the drug with ferrous ion (Fe^{2+}). The ability of anthracyclines to efficiently chelate Fe^{3+} ions has been extensively studied (Fiallo et al., 1999) because it is thought to be implied in this drug cardiotoxicity (Tokarska-Schlattner et al., 2006) and in oxidative destruction of DNA (Eliot et al., 1984). It has been established that, in the Fe^{3+}–DOX complex, the α-ketol group of the drug reduces iron to Fe^{2+} while being itself oxidized to semidione free radicals (Hasinoff, 1989; Malisza and Hasinoff, 1995). The oxidation products are able to stimulate a production of reactive oxygen species (ROS) that are more implied in the cardiotoxicity (Andreadou et al., 2007) than in the anticancer activity of the drug (Keizer et al., 1990). These considerations motivated our choice of ferrous ion rather than ferric ion to play the role of intermediate in the DOX–SPION binding. At the same time, particular care was taken to reduce the presence of free iron in the samples.

We obtained DOX-carrying SPION ferrofluids with properties favorable for magnetic drug targeting, i.e. drug loading of up to $14.6 \pm 0.5\%$ (defined below) and rapid release kinetics at physiological pH 7.4 (~85% DOX released in 1 h). It should be particularly underlined that this release provided free DOX and not DOX–iron complex. Furthermore, the biological evaluation of DOX-loaded SPION demonstrates that their cytotoxicity against MCF-7 cancer cells is not only preserved but, under certain conditions, is even increased compared to DOX solutions.

2. Experimental

2.1. Chemicals

Doxorubicin hydrochloride was purchased from TEVA Pharmaceuticals Ltd. (Puteaux, France). Potassium hydroxide solution was purchased from Prolabo (Fontenay-sous-Bois, France). Dimethylsulfoxide (DMSO), ferric nitrate, MTT and penicillin-streptomycin solution were furnished by Sigma–Aldrich (Saint-Quentin-Fallavier, France). Sodium acetate and tris-(hydroxymethyl)-aminomethane (Tris) were provided by Merck (Fontenay-sous-Bois, France). Anhydrous ferrous chloride, citric acid, Dulbecco's modified Eagle medium (DMEM), iron standard solution (titrisol), hydrochloric acid solution (trace analysis or analytical grade) and ferrous chloride ($FeCl_2{\cdot}4H_2O$) were purchased from Fisher Bioblock Scientific (Illkirch, France), and ferrous ammonium sulphate ($(NH_4)_2Fe(SO_4)_2{\cdot}6H_2O$) from Carlo Erba (Val de Reuil, France).

2.2. Preparation and characterization of citrate-stabilized ferrofluids of SPION

SPION were synthesized as aqueous ferrofluids by a coprecipitation of ferric and ferrous chlorides in alkaline medium followed by a surface oxidation by ferric nitrate and finally peptized in water, as described elsewhere (Chourpa et al., 2005). To increase the stability of the ferrofluid suspension at neutral pH, the SPION surface was treated with citrate ions by incubation in a 1.5-g/L citric acid solution under vigorous agitation for 2 h. Following this treatment, the ferrofluid pH was readjusted to 7.0 by addition of potassium hydroxide. The particles were then purified from excess citrate by 48 h dialysis (Float-a-Lyzer dialysis membrane, MWCO 8000, Interchim, France) against a 150-fold acceptor volume of distilled water.

The SPION concentration in ferrofluids was 0.56 g/L as estimated based on the measured iron concentration and considering that iron represents 71.5% of SPION (composed of 60% magnetite and 40% maghemite; Chourpa et al., 2005). The overall iron content ($Fe^{2+} + Fe^{3+}$) in the ferrofluids was 0.4 g/L as measured by atomic absorption spectrophotometry (SpectrAA-10 Plus spectrometer, Varian, France) using a calibration curve obtained with titrisol standard solution. Prior to these measurements, the particles were dissolved in HCl 6 M.

The hydrodynamic diameter of the particles was determined by DLS (dynamic light scattering) technique with an Autosizer 2c (Malvern Instruments, Orsay, France). The fine particle morphology was analysed by transmission electron microscopy (TEM) using a JEOL 1010 microscope (Jeol, Japan) at 88 kV. The samples were placed on a carbon coated copper grid and stained with 3% (w/v) uranyl acetate for TEM viewing.

2.3. Preparation and characterization of DOX–Fe^{2+} complex and of DOX–SPION ferrofluids

DOX–Fe^{2+} complex solutions of variable drug/iron molar ratio were obtained by adding an aqueous solution of ferrous ammonium sulphate ($(NH_4)_2Fe(SO_4)_2{\cdot}6H_2O$) to DOX in Tris buffer pH 7.6. The drug–iron complex used to load the nanoparticles was prepared with a 1.5-fold molar excess of Fe^{2+} over DOX. Then the DOX–Fe(II) complex was incubated in the dark with citrate-treated ferrofluid (total iron concentration 0.05 g/L), varying the mass ratio of DOX/SPION from 0.16 to 0.95 (w/w). After 15 min incubation, the drug-loaded SPION were harvested by centrifugation at $15{,}000 \times g$ for 15 min (4 °C). Finally, the nanoparticles were washed with ice-cold fresh aqueous buffer pH 7.6 and used immediately afterwards.

The DOX loading (%) was defined as the weight fraction of the drug in the final drug-loaded SPION. To measure the loaded drug, the particles were re-suspended for 20 min in acetate buffer pH 4.0, conditions that lead to dissociation of the DOX–Fe^{2+} complex and therefore to release of 100% of DOX (discussed below). The sample was then centrifuged and the DOX concentration in the supernatant was measured by means of UV–vis spectrophotometry (Anthélie Advanced Spectrophotometer, Secomam, France), using the DOX absorbance at 480 nm ($\varepsilon = 11{,}500\ cm^{-1}\ mol^{-1}\ L$, Fiallo et al., 1999). Each determination was performed in quadruplicate.

2.4. In vitro kinetics of drug release from DOX–SPION ferrofluids

To start the drug release, small aliquots (200 μL) of the drug-loaded ferrofluid (SPION concentration 0.17 g/L) were rapidly added to equal volumes (3.8 mL) of Tris buffer pH 7.4, thermostated at 37 °C and continuously shaken. At given time intervals, each tube was centrifuged (15,000 × *g* for 15 min, 4 °C), and the released drug concentration in the supernatant was determined from the intensity of the drug fluorescence at 556 nm (Hitachi F-4500 fluorescence spectrometer, excitation wavelength 500 nm, emission range 530–700 nm), using a calibration curve established previously. In parallel, the total amount of loaded doxorubicin was determined similarly, with an equal aliquot transferred into a buffer pH 4.0. Each experiment was performed in triplicate. This release method, i.e. shaking followed by centrifugation, was inspired by literature (Boonsongrit et al., 2008; Layre et al., 2006; Moreno et al., 2008; Zhang and Feng, 2006)

2.5. Cytotoxicity evaluation of DOX-loaded SPION ferrofluids

MCF-7 human breast carcinoma cells (American Type Culture Collection, LGC Promochem, Molsheim, France) were grown in DMEM supplemented with 5% foetal bovine serum and 100 UI/mL penicillin G and 100 μg/mL streptomycin at 37 °C in a humidified 5% CO_2 atmosphere.

For cytotoxicity assays, cells were seeded for 1 day in standard 96-well plates (Cellstar, Greiner Bio-One, Courtaboeuf, France) at 2×10^4 cells per well. Then the culture medium was discarded and the cells were treated for 24 h with 200 μL of medium containing different doxorubicin concentrations (0.3–8.6 μM), either as DOX solutions or as DOX–SPION suspensions (SPION content from 1.5 to 43.4 mg/L). For control cytotoxicity measurements, the cells were incubated with DOX-free ferrofluids of the same batch. On the other hand, cytotoxicity of DOX–Fe^{2+} complex solutions and of Fe^{2+} solutions was also studied (DOX concentrations between 0.3 and 8.6 μM, and Fe^{2+} concentrations between 0.3 and 10 μM).

Cell viability was determined using a tetrazolium dye (MTT) assay (Mosmann, 1983). The cells were rinsed thrice with potassium-buffered saline (PBS) pH 7.4 and incubated for 4 h in 100 μL of medium containing 0.5 g/L MTT. Then the medium was replaced by 100 μL of DMSO to dissolve the formazan crystals formed by viable cells. Absorbance was measured at 540 nm using a multiwell plate reader (Wallac Victor^2 1420 Multilabel Counter, Perkin Elmer, Courtaboeuf, France). The 50% inhibitory concentration (IC_{50}) was determined as the drug concentration that resulted in a 50% reduction in cell viability. All the experiments were performed in triplicate. Data analysis was performed using Origin 5.0 software (Integral Software, Paris, France).

3. Results and discussion

3.1. Characteristics of DOX–Fe(II) complex

Although free DOX possesses an intrinsic fluorescence, the DOX–iron complex is not fluorescent (data not shown). Thus, fluorescence can be used for the sensitive determination of free DOX. In contrast, although less sensitive than fluorimetry, UV–vis spectrophotometry is appropriate to study both free drug and drug–iron complex.

As pH increases beyond 7.5, the absorption spectra of DOX undergo significant changes (Fig. 2a): absorption maxima at 480 and 500 nm decrease and a new absorption maximum appears near 600 nm. These changes are related to deprotonation of the phenolic groups at positions C11 and C6 (pK_a 9.5 and 11.5, respectively; Razzano et al., 1990). On the other hand, iron(III) chelation by DOX is known to perturb in a similar way the UV–vis absorption spectra of the drug (Fiallo et al., 1999). This is consistent with the model where iron chelation involves the phenol groups at positions C11 and C6 (Fiallo et al., 1999). It is interesting to note that the absorption changes are more pronounced upon iron complexation than when the pH is increased.

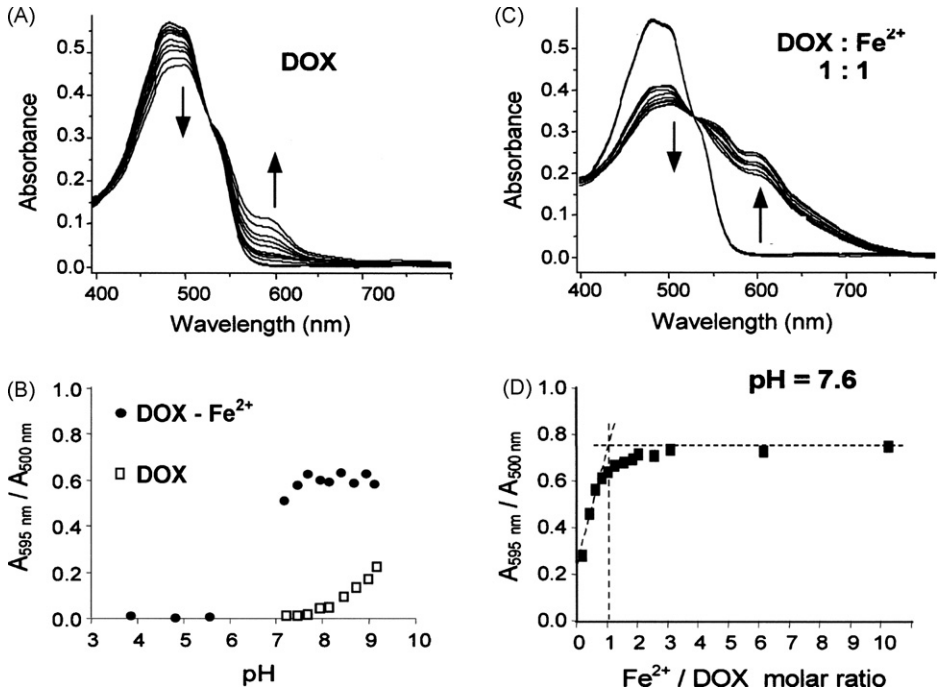

Fig. 2. UV–vis spectrophotometry data on DOX–Fe(II) complex: (a) changes in the DOX absorption spectra upon increasing pH from 4.0 to 9.2; no changes are observed below pH 7.2; (b) same as (a) for DOX in the presence of equimolar Fe^{2+} concentration; (c) pH dependence of DOX and DOX:Fe^{2+} 1:1 complex absorption spectra as monitored by the absorbance ratio ($A_{595\,nm}/A_{500\,nm}$); (d) spectrophotometric titration of the complex at pH 7.6 (Tris buffer) showing 1:1 stoichiometry.

The complex DOX–Fe^{2+} exhibits absorption spectra (Fig. 2b) similar to those of DOX–Fe^{3+}. To monitor the formation of the DOX–Fe^{2+} complex, one can use the ratio of the absorbances at 595 and 500 nm (Fig. 2c and d).

As can be seen in Fig. 2c, the DOX–Fe^{2+} complex is efficiently formed at neutral and basic pH, but is not observed at acidic pH. In the presence of iron, the great stability of the drug–iron complex leads to almost complete deprotonation of DOX at pH 7, i.e. significantly below the pK_a. In addition, at basic pH DOX is known to be unstable (Fiallo et al., 1999). Taking into account these considerations, we chose to prepare the DOX–Fe^{2+} complex at pH 7.6 (Tris buffer). At this pH, the iron chelation should preferentially imply the C11 phenolic group of doxorubicin. In agreement with this assumption, the spectrophotometric titration (Fig. 2d) shows that the stoichiometry of the complex at pH 7.6 is 1:1. This finding allows us to choose the optimal conditions for further complex preparation without a too large excess of free iron. Afterward, to pre-form the DOX–Fe^{2+} complex for loading onto ferrofluids, we will use a 1.5-fold iron/DOX molar ratio as sufficient to insure near-quantitative chelation of DOX.

3.2. Loading SPION ferrofluids with DOX using DOX–Fe^{2+} complex

The ferrofluids used in this study were found to consist of SPION with an average diameter of 8 ± 2 nm according to TEM (Fig. 3) and showed a sharp maximum of hydrodynamic diameter distribution around 20–22 nm in DLS (data not shown). According to previously described analysis by Raman spectroscopy (Chourpa et al., 2005) our SPION typically consisted of ~60% magnetite (Fe_3O_4) and ~40% maghemite (γ-Fe_2O_3) that constitute respectively the inner nucleus and the outer layer of each particle. The maghemite crystal is composed of Fe^{3+} and O^{2-} ions. Thus, the same doxorubicin functions implied in iron chelation could also favor the immobilization of the drug molecule directly on the iron oxide surface. However, preliminary experiments showed no significant adsorption of doxorubicin, neither on the native nor on the citrate-treated SPION. We suppose

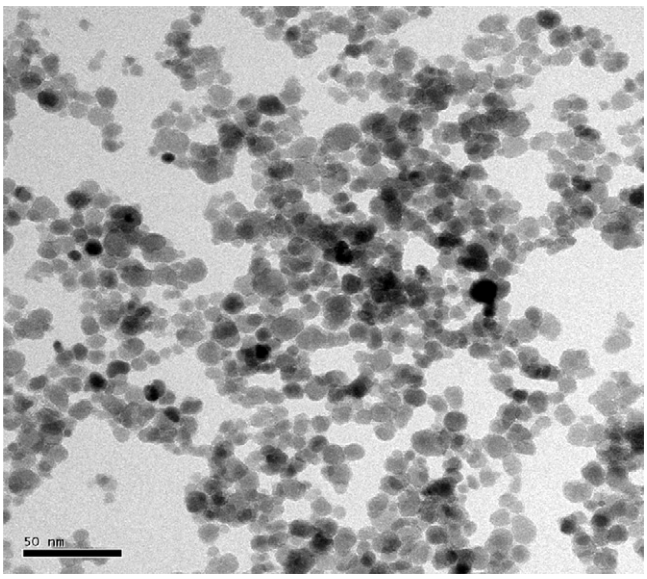

Fig. 3. TEM image of SPION described in the present study.

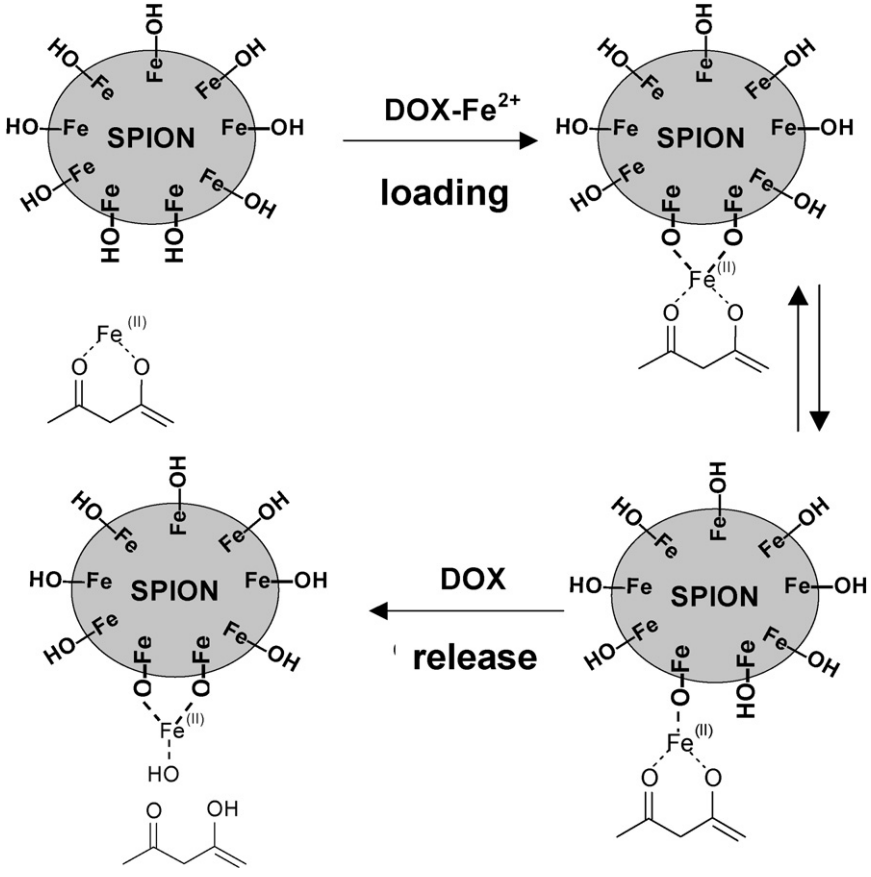

Fig. 4. Schematic diagram of DOX–Fe^{2+} binding to the SPION surface (pH 6–8) and of subsequent drug release.

that the interaction of DOX with iron on the nanoparticle surface is hindered by a layer of water and hydroxyl species.

To overcome this problem, we propose a novel method that consists in binding the drug to the particle surface using a pre-formed DOX–Fe^{2+} complex. In this case, the Fe^{2+} ion plays the role of an intermediate between DOX and particle (Fig. 4). As explained in the introduction, we preferred the use of Fe^{2+} over Fe^{3+} to avoid the undesirable oxidation of DOX.

From the very first experiments it was clear that incubation of SPION ferrofluids with pre-formed DOX–Fe^{2+} complex (pH 7.6, described in Section 2) leads to efficient DOX retention on the nanoparticles as revealed by a significant decrease of doxorubicin absorbance in the supernatant after SPION removal by centrifugation. For the DOX-loaded ferrofluids, the DLS analysis was perturbed because of the visible light absorption/emission of the drug. As expected, the DOX–SPION aspect in TEM was not different from that of citrated SPION.

To quantify the amount of DOX immobilized on the SPION (hereafter referred to as DOX loading, defined in Section 2), we measured the absorbance of the drug quantitatively released from the SPION in the buffer pH 4.0. The acidic aqueous environment induces instantaneous and complete desorption of the drug from the surface of the loaded SPION because the phenol protonation results in dissociation of the DOX–iron complex (Fig. 2c).

To optimise the protocols of drug binding on the ferrofluids, we studied DOX loading as a function of the amount of DOX initially used during incubation (Fig. 5a). For initial drug/SPION (w/w) ratios comprised between 0.16 and 0.95, the extent of DOX loading is rather high: from 5.4 ± 0.7 to 14.6 ± 0.5% (w/w). Thus, the novel method proposed in this work is particularly efficient. As far as we know, the drug loading of 14% exceeds the maximal loading values reported in literature up today (12%, Rudge et al., 2000).

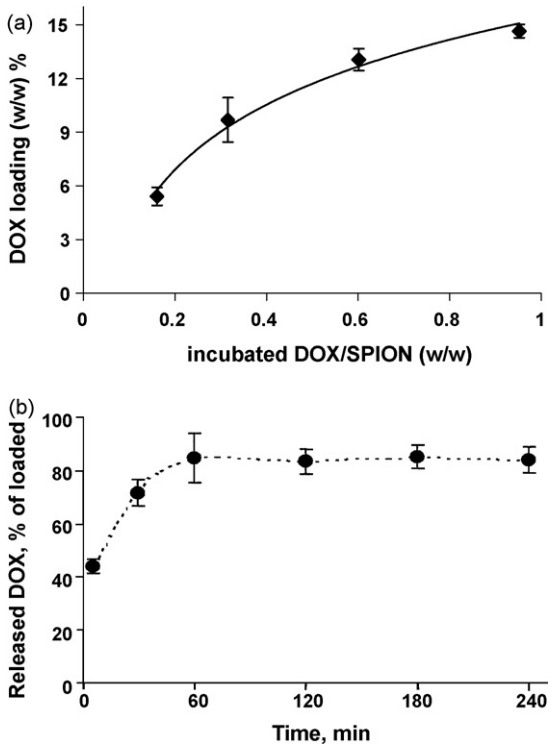

Fig. 5. Binding of DOX–Fe^{2+} complex to citrate-stabilized SPION: (a) DOX loading vs. initial drug/SPION weight ratio; (b) release of doxorubicin *in vitro* (Tris buffer pH 7.4) from drug-loaded SPION ferrofluids.

Furthermore, the shape of the curve in Fig. 5a suggests that the saturation was not attained yet. However, beyond a mass ratio of 1, any further increase in the amount of drug bound has to be paid by an unacceptable quantity of drug wasted. From this point of view, in the further studies of DOX release and activity we chose the protocol with a DOX/SPION (w/w) ratio of 0.31 upon incubation and providing nearly 9.7% (w/w) of DOX loaded (Fig. 5a).

3.3. *In vitro DOX release from DOX–SPION ferrofluids*

The *in vitro* release of DOX from loaded SPION ferrofluids was studied in Tris buffer pH 7.4 (pH of blood plasma) at 37 °C. At these conditions, the DOX–Fe^{2+} complex is favored by pH (Fig. 2c) and the drug is supposed to be gradually released from the SPION surface by a mechanism of hydrolysis (Fig. 5b).

As described in Section 2, each batch of DOX–SPION ferrofluids was divided in small aliquots to be analysed after different release times. After centrifugation, the concentration of DOX in the supernatant of each aliquot was calculated from the fluorescence emission intensity at 556 nm. The drug concentrations in these aliquots were too low (absorbance below 0.05) to be determined quantitatively by UV–vis spectroscopy. Nevertheless, the absorption spectra permitted to monitor qualitatively the spectra of released DOX.

The absorption spectra of the release medium correspond to that of free DOX (data not shown). Thus, the drug released at pH 7.4 is free and not in the form of a DOX–iron complex. At the same time, there seems to be no significant release of free iron from the nanoparticles, since otherwise it would also be detected through the characteristic UV–vis spectra of the DOX–iron complex. It appears that the chelate is bound to the SPION surface because of irreversible iron binding to the particle. This finding is consistent with results of Pang et al. who demonstrated that at neutral pH, there was a high affinity of iron to the SPION surface and no soluble iron was detected in ferrofluids (Pang et al., 2007). From a pharmaceutical point of view, this means that the cytotoxic activity of the DOX–SPION ferrofluids described below should not be assigned to released DOX–Fe^{2+} molecular complex or free iron. From an analytical point of view, this means that we can use fluorescence to quantify the drug released. The fact that the characteristic DOX fluorescence is observed in the release medium pH 7.4 indicates that the anthracycline chromophore is intact.

According to clinical experiences of Lübbe et al., a realistic duration of the treatment assisted with magnetic field should be comprised between 60 and 120 min (Lübbe et al., 1996b).

The release kinetics obtained in our study (Fig. 5b) demonstrates that the DOX–SPION binding is easily reversed at physiological pH. According to the fluorescence measurements, at pH 7.4, the DOX–SPION aqueous ferrofluids released 85 ± 9.1% of loaded DOX in 1 h and then the release curve attained a plateau. For comparison, the kinetics we observe with our DOX–SPION system are close to the results reported by Lübbe et al.; for epirubicin adsorbed onto polymer-coated iron oxide nanoparticles the desorption half-life was about 30 min, depending on physiological environment (pH, osmolarity, and temperature; Lübbe et al., 1996a). In our study, the DOX fraction of at least 6% not accounted for during the release experiments has been confirmed repeatedly. We believe that it may be in part explained by fluorescence quenching, namely due to phenomena like stacking of DOX molecules, that could appear on the SPION surface and persist after release.

With DOX–SPION system, the drug release is also pH-dependent: it accelerates with pH lowering and becomes almost instantaneous at pH 4.0. Such pH-dependence could be advantageous, since the relatively low pH in tumors will specifically stimulate the DOX release in the target site. Indeed, it is well

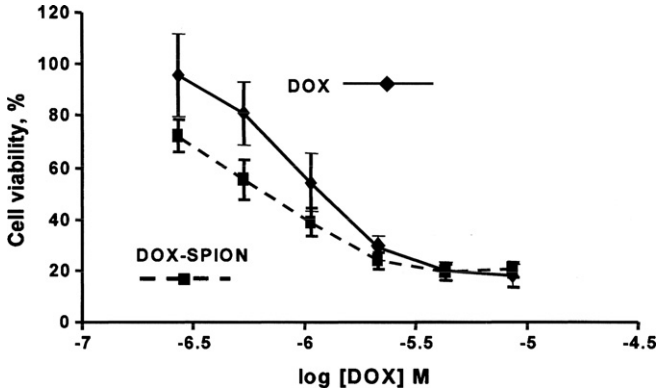

Fig. 6. *In vitro* cytotoxic activity profiles of DOX-loaded SPION ferrofluids (DOX–SPION) compared to drug in solution (DOX), when applied for 24 h on the MCF-7 cancer cells in culture. The differences are statistically significant for concentrations $\leq 10^{-6}$ M.

documented that the extracellular pH of tumors is more acidic (pH 5.7) than the blood and normal tissue pH 7.4 (Engin et al., 1995). In addition, if DOX–SPION are taken up by cells, the pH drops to pH 5.5–6.0 in endosomes and approaches pH 4.5–5.0 in lysosomes (Mellman et al., 1986). Therefore, DOX–SPION associates responsive to pH should selectively release their payload in tumor tissue or within cancer cells.

3.4. *In vitro* biological evaluation of DOX–SPION ferrofluids

We compared the biological activity of DOX solutions with that of DOX–SPION ferrofluids carrying the same amount of the drug by measuring their cytotoxicity on MCF-7 cancer cells. The related cytotoxicity profiles (cell viability after a 24 h treatment versus drug concentration) are shown in Fig. 6. At higher drug concentrations, both DOX and DOX–SPION have similar activity, while at lower drug concentrations, DOX–SPION kill more cancer cells. Therefore, within the DOX–SPION ferrofluids the *in vitro* cytotoxicity of DOX is not only preserved but even increased if compared at low-drug concentration range.

The IC_{50} values were determined to be 1.2 and 0.7 μM with DOX and DOX–SPION, respectively. It needs to be pointed out here that neither drug-free SPION ferrofluids nor iron solution (adjusted for the same iron concentration) produce any detectable cytotoxicity on MCF-7 cells (data not shown). This was in agreement with literature (Müller et al., 2007; Thorek and Tsourkas, 2008; Xu et al., 2006). On the other hand, there was no increase in cytotoxicity when the cells were treated with an extemporaneous mixture of SPION ferrofluid with DOX solution (used at DOX concentration below IC_{50}). Finally, the cytotoxic activity of DOX–Fe^{2+} solution was similar to that of DOX solution. These data indicate that the potent cytotoxicity observed above should be assigned to DOX-loaded SPION.

The increased cytotoxic activity of DOX–SPION could be due to the fact that the drug is released on the cellular membrane or maybe even delivered inside the cells by internalized nanoparticles. There are literature data confirming internalization of SPION by cells by optical microscopy (Schöpf et al., 2005) and electron microscopy (Wilhelm et al., 2003) both being used with rather high-particle concentrations (0.5–1.5 g/L). These concentrations were not applicable to DOX-loaded SPION because of their strong cytotoxicity. To address the mechanisms of action of such magnetic nanovectors, we are currently performing an extensive biological evaluation that will be the scope of the following publications of our group.

4. Conclusion

A new approach of binding and pH-sensitive release of DOX to SPION surfaces using a pre-formed DOX–Fe^{2+} complex is proposed and evaluated. This approach allows the preparation of DOX-loaded SPION ferrofluids carrying elevated amounts of drug. The drug release is rapid at physiological pH and accelerates in acidic medium (as found in tumor tissues and in cancer cells). The released DOX is free of iron and exhibits a cytotoxic activity at least as high as that of a drug solution. This fact, combined with the increased local drug concentrations expected from magnetic drug targeting, appears really promising for developing novel vectors for magnetically targeted chemotherapy on the basis of DOX–SPION.

Acknowledgments

This work was supported in part by grants from the Ligue Nationale contre le Cancer (Comités Indre-et-Loire, Loir-et-Cher, Indre). The authors thank E. Sarazin, K. Tessier and J.F. Fouquenet for technical assistance and are particularly grateful to Professor D. Bout (Université François Rabelais de Tours) for his help in the very first biological evaluation experiments.

References

Alexiou, C., Arnold, W., Klein, R.J., Parak, F.G., Hulin, P., Bergemann, C., Erhardt, W., Wagenpfeil, S., Lübbe, A.S., 2000. Locoregional cancer treatment with magnetic drug targeting. Cancer Res. 60, 6641–6648.

Alexiou, C., Jurgons, R., Seliger, C., Iro, H., 2006. Medical applications of magnetic nanoparticles. J. Nanosci. Nanotechnol. 6, 2762–2768.

Andreadou, I., Sigala, F., Iliodromitis, E.K., Papaefthimiou, M., Sigalas, C., Aligiannis, N., Savvari, P., Gorgoulis, V., Papalabros, E., Kremastinos, D.T., 2007. Acute doxorubicin cardiotoxicity is successfully treated with the phytochemical oleuropein through suppression of oxidative and nitrosative stress. J. Mol. Cell Cardiol. 42, 549–558.

Bast, A., Kaiserová, H., den Hartog, G.J.M., Haenen, G.R.M.M., van der Vijgh, W.J.F., 2007. Protectors against doxorubicin-induced cardiotoxicity: flavonoids. Cell Biol. Toxicol. 23, 39–47.

Berry, C.C., Curtis, A.S.G., 2003. Functionalisation of magnetic nanoparticles for applications in biomedicine. J. Phys. D: Appl. Phys. 36, R198–R206.

Boonsongrit, Y., Mitrevej, A., Mueller, B.W., 2008. Chitosan drug binding by ionic interaction. Eur. J. Pharm. Biopharm. 62, 267–274.

Chourpa, I., Douziech-Eyrolles, L., Ngaboni Okassa, L., Fouquenet, J.F., Cohen-Jonathan, S., Soucé, M., Marchais, H., Dubois, P., 2005. Molecular composition of iron oxide nanoparticles, precursors for magnetic drug targeting, as characterized by confocal Raman microspectroscopy. Analyst 130, 1395–1403.

Corot, C., Robert, P., Idée, J.M., Port, M., 2006. Recent advances in iron oxide nanocrystal technology for medical imaging. Adv. Drug Deliv. Rev. 58, 1471–1504.

Duguet, E., Vasseur, S., Mornet, S., Goglio, G., Demourgues, A., Portier, J., Grasset, F., Veverka, P., Pollert, E., 2006. Towards a versatile platform based on magnetic nanoparticles for *in vivo* applications. Bull. Mater. Sci. 29, 581–586.

Eliot, H., Gianni, L., Myers, C., 1984. Oxidative destruction of DNA by the adriamycin–iron complex. Biochemistry 23, 928–936.

Engin, K., Leeper, D.B., Cater, J.R., Thistlethwaite, A.J., Tupchong, L., McFarlane, J.D., 1995. Extracellular pH distribution in human tumors. Int. J. Hyperther. 11, 211–216.

Fiallo, M.M.L., Garnier-Suillerot, A., Matzanke, B., Kozlowski, H., 1999. How Fe^{3+} binds anthracycline antitumour compounds. The myth and the reality of a chemical sphinx. J. Inorg. Biochem. 75, 105–115.

Hasinoff, B.B., 1989. Self-reduction of the iron(III)–doxorubicin complex. Free Radic. Biol. Med. 7, 583–593.

Hoke, E.M., Maylock, C.A., Shacter, E., 2005. Desferal inhibits breast tumor growth and does not interfere with the tumoricidal activity of doxorubicin. Free Radic. Biol. Med. 39, 403–411.

Inoh, K., Muramatsu, H., Torii, S., Ikematsu, S., Oda, M., Kumai, H., Sakuma, S., Inui, T., Kimura, T., Muramatsu, T., 2006. Doxorubicin-conjugated anti-midkine monoclonal antibody as a potential anti-tumor drug. Jpn. J. Clin. Oncol. 36, 207–211.

Jain, T.K., Morales, M.A., Sahoo, S.K., Leslie-Pelecky, D.L., Labhasetwar, V., 2005. Iron oxide nanoparticles for sustained delivery of anticancer agents. Mol. Pharm. 2, 194–205.

Keizer, H.G., Pinedo, H.M., Schuurhus, G.J., Joenje, H., 1990. Doxorubicin (adriamycin): a critical review of free radical-dependent mechanisms of cytotoxicity. Pharmacol. Ther. 47, 219–231.

Layre, A., Couvreur, P., Chacun, H., Richard, J., Passirani, C., Requier, D., Benoit, J.P., Gref, R., 2006. Novel composite core-shell nanoparticles as busulfan carriers. J. Control Release 111, 271–280.

Lo, E.H.K., Ooi, V.E.L., Fung, K.P., 2002. Circumvention of multidrug resistance and reduction of cardiotoxicity of doxorubicin *in vivo* by coupling it with low density lipoprotein. Life Sci. 72, 677–687.

Lübbe, A.S., Alexiou, C., Bergemann, C., 2001. Clinical applications of magnetic drug targeting. J. Surg. Res. 95, 200–207.

Lübbe, A.S., Bergemann, C., Huhnt, W., Fricke, T., Riess, H., Brock, J.W., Huhn, D., 1996a. Preclinical experiences with magnetic drug targeting: tolerance and efficacy. Cancer Res. 56, 4694–4701.

Lübbe, A.S., Bergemann, C., Riess, H., Schriever, F., Reichardt, P., Possinger, K., Matthias, M., Dorken, B., Herrmann, F., Gurtler, R., Hohenberger, P., Haas, N., Sohr, R., Sander, B., Lemke, A.J., Ohlendorf, D., Huhnt, W., Huhn, D., 1996b. Clinical experiences with magnetic drug targeting: a phase I study with 4′-epidoxorubicin in 14 patients with advanced solid tumors. Cancer Res. 56, 4686–4693.

Malisza, K.L., Hasinoff, B.B., 1995. Production of hydroxyl radical by iron(III)–anthraquinone complexes through self-reduction and through reductive activation by the xanthine oxidase/hypoxanthine system. Arch. Biochem. Biophys. 321, 51–60.

Mellman, I., Fuchs, R., Helenius, A., 1986. Acidification of the endocytic and exocytic pathways. Annu. Rev. Biochem. 55, 700–773.

Moghimi, S.M., Kissel, T., 2006. Preface. Particulate nanomedicines. Adv. Drug. Deliv. Rev. 58, 1451–1455.

Moreno, D., Tros de Ilarduya, C., Bandrés, E., Buñuales, M., Azcona, M., García-Foncillas, J., Garrido, M.J., 2008. Characterization of cisplatin cytotoxicity delivered from PLGA-systems. Eur. J. Pharm. Biopharm. 68, 503–512.

Mosmann, T., 1983. Rapid colorimetric assay for cellular growth and survival: application to proliferation and cytotoxicity assays. J. Immunol. Meth. 65, 55–63.

Müller, K., Skepper, J.N., Posfai, M., Trivedi, R., Howarth, S., Corot, C., Lancelot, E., Thompson, P.W., Brown, A.P., Gillard, J.H., 2007. Effect of ultrasmall superparamagnetic iron oxide nanoparticles (Ferumoxtran-10) on human monocyte-macrophages in vitro. Biomaterials 28, 1629–1642.

Mykhaylyk, O., Dudchenko, N., Dudchenko, A., 2005. Doxorubicin magnetic conjugate targeting upon intravenous injection into mice: high gradient magnetic field inhibits the clearance of nanoparticles from the blood. J. Magn. Magn. Mater. 293, 473–482.

Neuberger, T., Schöpf, B., Hofmann, H., Hofmann, M., von Rechenberg, B., 2005. Superparamagnetic nanoparticles for biomedical applications: possibilities and limitations of a new drug delivery system. J. Magn. Magn. Mater. 293, 483–496.

Ngaboni Okassa, L., Marchais, H., Douziech-Eyrolles, L., Hervé, K., Cohen-Jonathan, S., Munnier, E., Soucé, M., Linassier, C., Dubois, P., Chourpa, I., 2007. Optimization of iron oxide nanoparticles encapsulation within poly(D,L-lactide-co-glycolide) sub-micron particles. Eur. J. Pharm. Biopharm. 67, 31–38.

Pang, S.C., Chin, S.F., Anderson, M.A., 2007. Redox equilibria of iron oxides in aqueous-based magnetite dispersions: effect of pH and redox potential. J. Magn. Magn. Mater. 311, 94–101.

Petit, T., 2004. Anthracycline-induced cardiotoxicity. Bull. Cancer 91, 159–165.

Razzano, G., Rizzo, V., Vigevani, A., 1990. Determination of phenolic ionization constants of anthracyclines with modified substitution pattern of anthraquinone chromophore. Farmaco 45, 215–222.

Rudge, S.R., Kurtz, T.L., Vessely, C.R., Catterall, L.G., Williamson, D.L., 2000. Preparation, characterization, and performance of magnetic iron–carbon composite microparticles for chemotherapy. Biometerials 21, 1411–1420.

Schöpf, B., Neuberger, T., Schulze, K., Petri, A., Chastellain, M., Hoffmann, M., Hoffmann, H., von Rechenberg, B., 2005. Methodology description of cellular uptake of PVA coated superparamagnetic iron oxide nanoparticles (SPION) in synovial cells of sheep. J. Magn. Magn. Mater. 293, 411–418.

Tokarska-Schlattner, M., Zaugg, M., Zuppinger, C., Wallimann, T., Schlattner, U., 2006. New insights into doxorubicin-induced cardiotoxicity: the critical role of cellular energetics. J. Mol. Cell Cardiol. 41, 389–405.

Torchilin, V.P., 2006. Multifunctional nanocarriers. Adv. Drug. Deliv. Rev. 58, 1532–1555.

Thorek, D.L.J., Tsourkas, A., 2008. Size, charge and concentration dependent uptake of iron oxide particles by non-phagocytic cells. Biomaterials 29, 3583–3590.

Wilhelm, C., Billotey, C., Roger, J., Pons, J.N., Bacri, J.C., Gazeau, F., 2003. Intracellular uptake of anionic superparamagnetic nanoparticles as a function of their surface coating. Biomaterials 24, 1001–1011.

Xu, Z.P., Zeng, Q.H., Lu, G.Q., Yu, A.B., 2006. Inorganic nanoparticles as carriers for efficient cellular delivery. Chem. Eng. Sci. 61, 1027–1040.

Zhang, J., Misra, R.D.K., 2007. Magnetic drug-targeting carrier encapsulated with thermosensitive smart polymer: core-shell nanoparticles carrier and drug release response. Acta Biomater. 3, 838–850.

Zhang, Z., Feng, S.-S., 2006. The drug encapsulation efficiency, in vitro drug release, cellular uptake and cytotoxicity of paclitaxel-loaded poly(lactide)–tocopheryl polyethylene glycol succinate nanoparticles. Biomaterials 27, 4025–4033.